

Temperature dependence of interlayer coupling in perpendicular magnetic tunnel junctions with GdO_x barriers

T. Newhouse-Illige¹, Y. H. Xu¹, Y. H. Liu², S. Huang¹, H. Kato¹, C. Bi¹,
M. Xu¹, B. J. LeRoy¹ and W. G. Wang^{1,*}

- 1) Department of Physics, University of Arizona, Tucson, Arizona 85721, USA
- 2) Quantum Condensed Matter Division, Oak Ridge National Laboratory, Oak Ridge, Tennessee 37831, USA

Perpendicular magnetic tunnel junctions with GdO_x tunneling barriers have shown a unique voltage controllable interlayer magnetic coupling effect. Here we investigate the quality of the GdO_x barrier and the coupling mechanism in these junctions by examining the temperature dependence of the tunneling magnetoresistance and the interlayer coupling from room temperature down to 11 K. The barrier is shown to be of good quality with the spin independent conductance only contributing a small portion, 14%, to the total room temperature conductance, similar to AlO_x and MgO barriers. The interlayer coupling, however, shows an anomalously strong temperature dependence including sign changes below 80 K. This non-trivial temperature dependence is not described by previous models of interlayer coupling and may be due to the large induced magnetic moment of the Gd ions in the barrier.

*wggwang@physics.arizona.edu

Spintronics^{1,2}, storing data with spin instead of charge, has been increasingly used for new computing devices. Taking advantage of the electron's spin degree of freedom in addition to its charge allows for non-volatile memory³, logic⁴, and sensor⁵ devices with low energy requirements. The magnetic tunnel junction (MTJ)⁶⁻¹⁰ is one of the most important functional units for these applications, where the information can be encoded in different resistive states. In general, MTJs can be switched with a magnetic field, a spin-polarized current by spin transfer torques (STT)^{11,12}, or a pure spin current by spin-orbit torques (SOT)^{13,14}. It is also possible to change the state of an MTJ with voltage¹⁵ for lower-power operation and easier integration with CMOS technologies. In MTJs with perpendicular magnetic anisotropy (pMTJ), the resistance can be switched through the combination of voltage controlled magnetic anisotropy (VCMA) and STT¹⁶. Subsequently, it has been demonstrated that pMTJs can be switched precessionally in a sub-nanosecond time scale by the effective in-plane field generated by the VCMA effect¹⁷⁻¹⁹. In addition, pMTJs can be manipulated by using voltage to control the interlayer coupling between the soft and hard ferromagnetic (FM) layers. This voltage controlled interlayer coupling (VCIC) effect was proposed theoretically²⁰⁻²³ and demonstrated recently in pMTJs with a GdO_x barrier, where the interlayer coupling field (H_{IC}) can be reversibly and deterministically controlled by voltage²⁴.

The nature of the interlayer coupling in GdO_x-pMTJs is of great interest itself. Generally, the observation of antiferromagnetic (AFM) coupling is more significant because a FM coupling could simply be due to the existence of pinholes in the barrier. A few models have been proposed to explain the coupling in MTJs with either in-plane magnetic anisotropy or perpendicular magnetic anisotropy (PMA). AFM interactions in an MTJ can be mediated by direct exchange coupling²⁵, described by wave function quantum interferences due to spin-dependent reflections at the FM/NM interfaces²⁶ or by the torques exerted by spin-polarized conduction electrons²⁷. In MgO-based MTJs with large tunneling magnetoresistance (TMR), indirect coupling mediated through oxygen vacancies within the barrier has been shown to be responsible for the observed AFM coupling²⁸. Finally, the AFM coupling in spin-valves and MTJs with PMA has been described by a roughness induced orange-peel magnetostatic coupling^{29,30}.

To evaluate the quality of the GdO_x barrier and understand the interlayer coupling mechanism, we investigate the temperature dependence of GdO_x-based pMTJs from room temperature (RT) down to 11 K. The spin-independent tunneling contributes only a small portion to the total conductance, similar to AlO_x and MgO based junctions, indicating a high quality barrier. More interestingly, H_{IC} shows a strong temperature dependence, even changing sign below 80 K. This behavior has not been accounted for in existing models, suggesting that the interlayer coupling in GdO_x-pMTJs is strongly linked to the magnetic properties of the GdO_x barrier.

Samples for this study were fabricated by magnetron sputtering in a 12 source UHV system with a base pressure of 10^{-9} Torr. The sample structure is Si/SiO₂/Ta(8 nm)/Ru(10 nm)/Ta(7 nm)/Co₂₀Fe₆₀B₂₀(0.7-0.9 nm)/GdO_x(1-3.5 nm)/Co₂₀Fe₆₀B₂₀(1.5-1.6 nm)/Ta(7 nm)/Ru(20 nm). The layers were deposited under similar conditions as those used for fabricating MgO-pMTJs where TMR above 200% has been obtained at RT³¹. All layers were deposited with DC sputtering. The GdO_x tunneling barrier was deposited by reactively sputtering of Gd target in

Ar+O₂ atmosphere. After deposition, samples were patterned, using standard photolithography and ion etch procedures³², into circular shapes with diameters (D) between 3 and 20 μm and a four wire contact geometry. Samples were measured on a custom probe station for RT measurements prior to wire bonding for temperature dependent measurements in an ARS sample-in-vapor cryostat with an external electromagnet. Although thick gadolinium oxide films exhibit a cubic Gd₂O₃ crystallization³³, the thin oxide layers in our MTJ samples are amorphous as revealed by the previous TEM study²⁴, and the oxidation state has not been precisely determined; therefore, the barrier is referred to here as GdO_x. The TEM study further revealed the interface between GdOX and CoFeB to be generally quite smooth, similar to what observed in AlO_x/CoFeB and MgO/CoFeB junctions²⁴.

Ferromagnetic layers in contact with gadolinium oxide have been shown to exhibit many unique voltage controllable magnetic properties. Due to the large ionic mobility of oxygen in GdO_x, it has been shown that voltage applied across a GdO_x/FM interface can modify the speed of domain wall motion, the magnetic saturation (M_s) and the anisotropy field (H_K), even to the degree of changing the orientation of the magnetic anisotropy between in-plane and perpendicular³³⁻³⁵. GdO_x was actually one of the first barriers used in the pioneering MTJ studies, where TMR was successfully observed at low temperature in junctions with in-plane magnetic anisotropy^{36,37}. In the current study, room temperature TMR up to 15% was obtained in pMTJs with the use of an improved MTJ structure and CoFeB electrodes²⁴. Representative TMR curves from these pMTJs at both RT (black) and 11 K (red) are displayed in Fig. 1, TMR being defined as (R_{AP} – R_P)/R_P where R_{AP} and R_P are the resistance in the antiparallel and parallel states, respectively. Both TMR curves show sharp resistance switchings and flat antiparallel plateaus as expected with pMTJs. Both the TMR and switching fields (H_C) increase considerably with the decrease in temperature as anticipated by previous results^{8,10,38,39}. Additionally, both temperatures show a TMR curve symmetric about zero field as expected. Although bulk Gd₂O₃ shows antiferromagnetic ordering, its Neel temperature is below 4 K⁴⁰, lower than any of our testing conditions. All figures in this report correspond to a representative sample with a core structure of Co₂₀Fe₆₀B₂₀(0.85 nm)/GdO_x(2.5 nm)/Co₂₀Fe₆₀B₂₀(1.5 nm) except where noted. All other samples with different GdO_x and/or CoFeB thicknesses show similar trends.

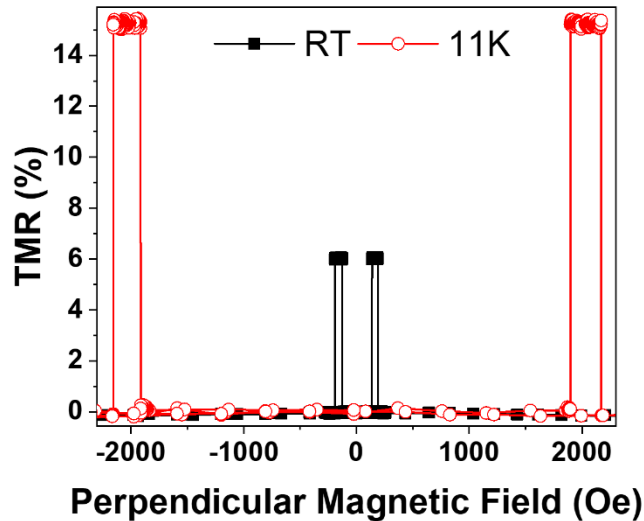


FIG. 1. TMR curves of a representative sample at RT (solid black) and 11 K (open red).

The increase in TMR at low temperature is illustrative of a tunneling mechanism with a spin-dependent contribution and a spin-independent contribution in the style of the two current model described by Shang *et al.*⁴¹. Following their model,

$$G(\theta) = G_T \{1 + P_1 P_2 \cos(\theta)\} + G_{SI} \quad (1)$$

where the first term is the spin-dependent tunneling and the second term, G_{SI} , is the spin-independent conductance. The temperature dependence of G_T , the direct elastic tunneling prefactor, is given by $G_T = G_0 CT / \sin(CT)$, with G_0 a constant and $C = 1.378 \times 10^{-4} d / \sqrt{\phi}$, d being the barrier width in Å and ϕ the barrier height in eV. Rewriting equation (1) for symmetric FM electrodes, the standard TMR formula of Julliere⁴² can be rewritten as $TMR = 2P^2 / (1 + P^2 + G_{SI}/G_T)$, where P is the polarization of the CoFeB electrodes. The polarization is assumed to vary with temperature in the same way as the magnetization such that, $P = P_0(1 - \alpha T^{3/2})$.

Figure 2(a) shows that the conductivity of both the parallel (red) and antiparallel (black) states decreases with temperature. Looking at the conductance difference, $\Delta G = G_P - G_{AP}$, with G_P (G_{AP}) being the conductance in the parallel (antiparallel) state, we can investigate only the spin-dependent conductance, since plugging $\theta = 0$ and π into equation (1) and subtracting gives

$$\Delta G = 2G_T P^2 = 2G_0 P_0^2 (1 - \alpha T^{3/2})^2 CT / \sin(CT) \quad (2)$$

Fitting ΔG data to equation (2) gives P_0 and α equal to 0.521 and $6.30 \times 10^{-5} \text{ K}^{-3/2}$, respectively. This value of α is in the expected range based on previous MTJs with MgO ⁴³ and AlO_x barriers⁴⁴.

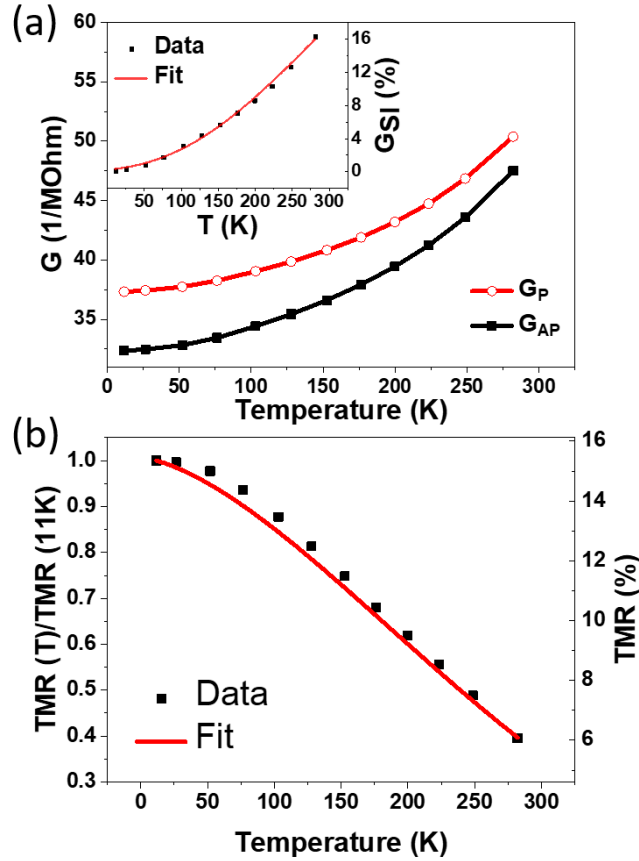


FIG. 2. (a) Conductance of the parallel (open red) and antiparallel (solid black) states. Inset. G_{SI} normalized to G_P , data (points) and fit (solid line). (b) The temperature dependence of the TMR, data (points) and fit (solid line).

The inset of Fig. 2(a) shows the temperature dependence of G_{SI} . Assuming G_{SI} is from conduction through localized defect hopping, which is mediated by coupling to phonons and so is strongly temperature dependent, we can model its temperature dependence. Under this assumption, G_{SI} takes the form^{45,46} $G_{SI} = \sum_N \sigma_N T^{(N-[2/(N+1)])}$, where N is the number of defect states involved in the hopping. The solid line in the inset of Fig. 2(a) shows that G_{SI} is well fit by $\sigma_1 + \sigma_2 T^{1.33} + \sigma_3 T^{2.5}$ with $\sigma_1 = 6.2 \cdot 10^{-8} \Omega^{-1}$, $\sigma_2 = 1.1 \cdot 10^{-9} \Omega^{-1} K^{-1.33}$, and $\sigma_3 = 4.5 \cdot 10^{-12} \Omega^{-1} K^{-2.5}$. From this, it can be seen that the defect hopping at RT is strongly dominated by hopping through three impurity states. The quality of the barrier can be estimated by examining the proportion of the total conductance contributed by G_{SI} at RT. The GdO_x -pMTJs investigated here have a G_{SI} contribution of about 14% of the total conductance at RT. In MTJs where a large number of defect states were present in the barrier, much larger G_{SI} was reported⁴⁷. Here the G_{SI} contribution in GdO_x is similar to the range obtained with AlO_x ^{41,44} and MgO ⁴³, 12-20%, indicating GdO_x can serve as a high-quality tunneling barrier with low defect states. Therefore, a much higher TMR could possibly be achieved with a crystalline Gd_2O_3 barrier, as demonstrated in the case of MgO ⁴⁸ and Al_2O_3 ⁴⁹. Now that we have the temperature dependence of G_T and G_{SI} , we are ready to compare our TMR data to that of the model. Figure 2(b) shows that our data is

well described by Equation 1 and that the model is sufficient to describe the tunneling in the GdO_x MTJs.

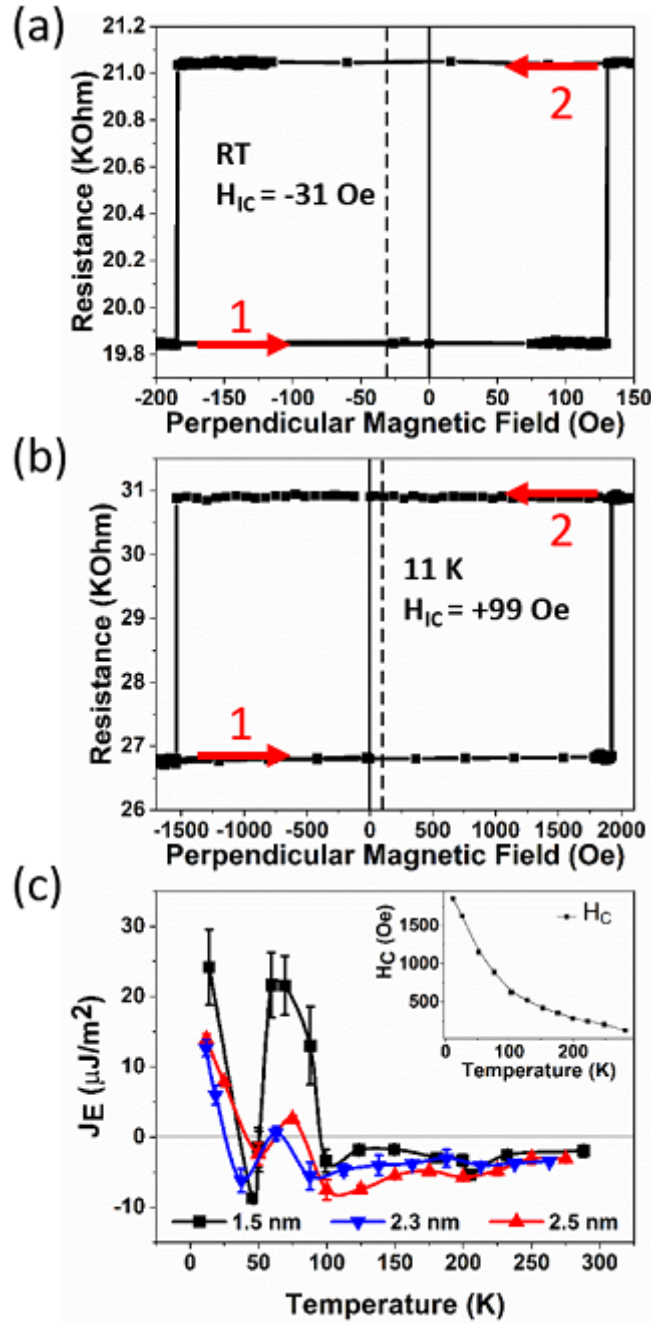


FIG. 3. (a) Minor TMR loop at RT, $H_{IC} = -31$ Oe. (b) Minor TMR loop at 11 K, $H_{IC} = +99$ Oe, dotted lines indicate the center of the loop for defining the H_{IC} and arrows indicate the sweeping direction of the magnetic field, (c) Interlayer coupling energy vs. T showing a non-trivial temperature dependence for three thicknesses of GdO_x tunneling barrier. Error bars come from averaging repeated loop measurements at each temperature. Inset. Positive switching field vs. T from RT down to 11 K showing a smooth increase for the 2.5 nm sample. The lines are a guide for the eye.

In addition to the full TMR loops, minor TMR loops were measured at each temperature by switching the soft FM layer while the hard layer magnetization remained pointing down. From the minor loop, the H_{IC} can be measured from the shift of the loop along the magnetic field axis. If the minor loop is centered about a positive (negative) field, the system is said to be ferromagnetically (antiferromagnetically) coupled and prefers to be in a parallel (antiparallel) state when no magnetic field is applied. Figures 3(a) and 3(b) show the minor loops of the same GdO_x -pMTJ at RT and 11 K, respectively. At RT, this pMTJ shows a H_c of 157 Oe and a H_{IC} of -31 Oe, consistent with the previous report²⁴. Notably, when cooled to 11 K, the H_{IC} changed sign to be +99 Oe, accompanied by an increase of H_c to 1730 Oe.

Previously, interlayer coupling has been studied in many systems, including spinvalves^{50,51} and MTJs with both in-plane^{25,28,52} and perpendicular anisotropy^{53,54}. The wide range of systems in which coupling has been observed has led to several theories describing its origin in MTJs. Bruno²⁶ described the coupling in all metallic spinvalves based on spin-dependent reflections at the boundaries of the FM layers. He then extended his theory to insulating MTJs with the inclusion of an imaginary Fermi momentum in the barrier. According to Bruno's theory, the coupling strength across an insulating barrier should increase with temperature following a $CT/\sin(CT)$ dependence and never change sign. This temperature dependence was seen experimentally in junctions based on amorphous Si and SiO_2 barriers⁵⁵ but does not explain the sign change seen between Figs. 3(a) and 3(b).

In MgO based MTJs with large TMR (in-plane magnetic anisotropy), another mechanism has been shown by Katayama *et al.*²⁸ where the coupling is mediated through oxygen vacancies in the MgO barrier. Following the theory by Zhuravlev *et al.*⁵⁶, the oxygen vacancies act as impurity states in the barrier that mediate coupling through the so called F center resonance. This coupling is shown to be AFM if the energy level of the impurity state lies at the Fermi energy. This model predicts a smooth strengthening of the coupling with decreasing temperature, which is opposite to the Bruno model. In a subsequent study by Yang *et al.*⁵⁷, a sign change of H_{IC} was predicted when the distribution of oxygen vacancies within the barrier was modified.

The interlayer coupling in pMTJs has been investigated less than in-plane MTJs, in part due to the larger difficulty involved with growing MTJs with out-of-plane easy axes. The first observation of AFM coupling in a pMTJ was made by Nistor *et al.*⁵³ in Co/MgO/Co junctions. Later this AFM coupling was partly explained by a model developed by Moritz *et al.*²⁹. In this model, correlated roughness at the FM interfaces induces orange-peel type Neel coupling⁵⁸. Coupling of this type is strongly dependent on the magnetic anisotropy energy. For PMA electrodes, a low anisotropy leads to FM coupling, while a larger PMA gives rise to AFM coupling. Additionally, in the AFM coupling regime, stronger PMA leads to a stronger coupling strength. An image showing the topography at the top of the GdO_x layer is displayed in Fig. 4. In agreement with previous TEM findings²⁴, this shows a smooth layer with RMS roughness of 0.130 nm. In our previous study, a smaller H_{IC} was observed when the PMA of the MTJ was increased by annealing at a higher temperature,²⁴ which is an indication that the AFM coupling observed in GdO_x -pMTJs is not described by the Moritz model. As pointed out by Nistor³⁰, however, the reduction of the AFM coupling after annealing at a higher temperature could be a result of reduced roughness. The measurement of H_{IC} from a single sample at different

temperatures provides critical information for understanding the coupling in GdO_x-pMTJs. According to the Moritz model, with a fixed roughness, the AFM coupling should get stronger at 11 K due to the larger PMA³⁹, which is not consistent with Figs. 3(a) and 3(b).

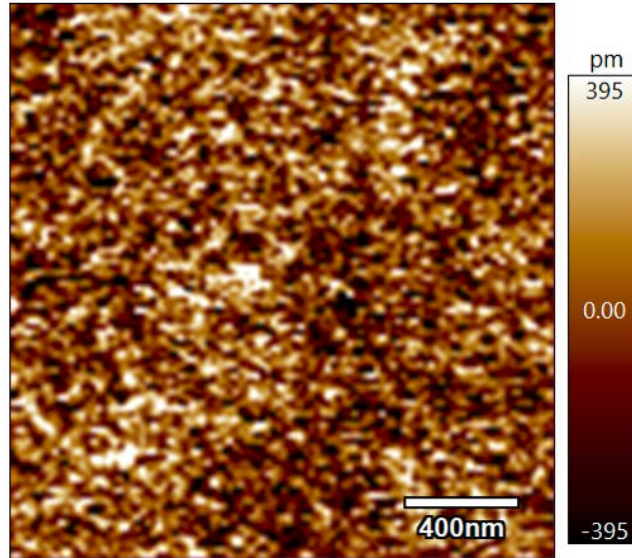


FIG. 4. Atomic force microscopy topography image of the GdO_x barrier layer.

Figure 3(c) shows the detailed temperature dependence of the interlayer coupling energy $J_e = 1/2 H_{IC} M_s t_m$ from RT down to 11 K for three GdO_x thicknesses. Where the saturation magnetization, M_s is assumed to follow the temperature dependence of spin wave excitations, $M_s = M_0(1 - \alpha T^{3/2})$ and t_m is the combined thickness of the hard and soft magnetic layers. Although it is hard to tell if there is a consistent dependence of the transition temperature on the GdO_x thickness with the current resolution of the data points, it is clear that the temperature dependence of J_E follows the same trend for all GdO_x thicknesses. All thicknesses show a non-trivial dependence that is not reflected by previous models and does not match any previous experimental data from other MTJ systems. Similarly, the J_E does not follow the smooth temperature dependence of the switching field as shown in the inset of Fig. 3(c), further confirming that it is not following the trend of the sample's PMA. In addition to the large magnitude and sign change shown between RT and 11 K in Figs. 3(a) and 3(b), there is a complex temperature dependence at intermediate temperatures, including multiple switches between AFM and FM coupling states, as shown in Fig. 3(c). Another possible explanation for the change in sign of H_{IC} at certain temperatures could be a reversal of the hard and soft FM layers as examined by Feng et al.⁵⁹ This possibility was explored however the crossover of the switching fields was not seen in our samples. In addition, we see no temperatures at which TMR curves do not exhibit sharp switches and a well-defined antiparallel state.

This unprecedented behavior of the interlayer coupling in GdO_x-pMTJs may be due to the large proximity effect⁶⁰ induced magnetic moment of the Gd ions in the barrier.²⁴ The induced magnetic moment of the Gd is found to be antiferromagnetically coupled to the FM electrodes and exhibits two distinct switchings that correspond to the MTJ switching fields, suggesting that they are magnetically coupled to both electrodes separately²⁴. If the coupling in

our GdO_x-pMTJs is mediated through the proximity magnetism of the GdO_x barrier, it could have a much more complex dependence on temperature than that predicted by earlier models. Previous studies have shown that the H_{IC} becomes negligibly small for thick enough barriers, generally vanishing for barriers thicker than 1 to 2 nm^{28,30,57}. The magnetic moment of the Gd ions may also explain why the coupling in our system extends to much thicker barriers than previously demonstrated. The effective barrier thickness may be significantly smaller than the thickness of the GdO_x if the proximity effect magnetizes a significant portion of each side of the barrier. A polarized neutron study is underway to investigate the thickness dependence of this proximity induced magnetism.

In summary, we have investigated the temperature dependence of GdO_x based pMTJs from RT down to 11 K. Similar to AlO_x and MgO based junctions, the spin-independent conductance contributes a only small proportion to the total conduction, indicative of a high-quality barrier. The most interesting result is that the H_{IC} shows a non-trivial temperature dependence, including changing sign below 80 K. This behavior is not characteristic of any of the existing models, suggesting that the interlayer coupling in GdO_x-pMTJs is mediated through the unique magnetic properties of the GdO_x tunneling barrier.

Acknowledgments

This work was supported in part by C-SPIN, one of six centers of STARnet, a Semiconductor Research Corporation program, sponsored by MARCO and DARPA, and by the National Science Foundation through ECCS-1554011 and ECCS-1607911. Work at ORNL was supported by the Division of Scientific User Facilities of the Office of Basic Energy Sciences (BES), U.S. Department of Energy (DOE). All Cypher AFM images and data were collected in the W.M. Keck Center for Nano-Scale Imaging in the Department of Chemistry and Biochemistry at the University of Arizona. This material is based upon work supported by the National Science Foundation under Grant Number 1337371.

References

1. Wolf, S. A., Awschalom, D. D., Buhrman, R. A., Daughton, J. M., von Molnár, S., Roukes, M. L., Chtchelkanova, A. Y. & Treger, D. M. Spintronics: a spin-based electronics vision for the future. *Science* **294**, 1488–95 (2001).
2. Žutić, I., Fabian, J. & Das Sarma, S. Spintronics: Fundamentals and applications. *Rev. Mod. Phys.* **76**, 323–410 (2004).
3. Gallagher, W. J. & Parkin, S. S. P. Development of the magnetic tunnel junction MRAM at IBM: From first junctions to a 16-Mb MRAM demonstrator chip. *IBM J. Res. Dev.* **50**, 5–23 (2006).
4. Prejbeanu, I. L., Bandiera, S., Alvarez-Hérault, J., Sousa, R. C., Dieny, B. & Nozières, J.-P. Thermally assisted MRAMs: ultimate scalability and logic functionalities. *J. Phys. D. Appl. Phys.* **46**, 74002 (2013).
5. Naik, V. B., Meng, H., Liu, R. S., Luo, P., Yap, S. & Han, G. C. Electric-field tunable magnetic-field-sensor based on CoFeB/MgO magnetic tunnel junction. *Appl. Phys. Lett.* **104**, 232401 (2014).
6. Moodera, J. S. and Kinder, Lisa R. and Wong, Terrilyn M. and Meservey, R. Large Magnetoresistance at Room-Temperature in Ferromagnetic Thin-Film Tunnel-Junctions. *Phys. Rev. Lett.* **74**, 3273–3276 (1995).
7. Miyazaki, T. & Tezuka, N. Giant magnetic tunneling effect in Fe / Al₂O₃ / Fe junction. *J. Magn. Magn. Mater.* **139**, 94–97 (1995).
8. Parkin, S. S. P., Kaiser, C., Panchula, A., Rice, P. M., Hughes, B., Samant, M. & Yang, S. H. Giant tunnelling magnetoresistance at room temperature with MgO (100) tunnel barriers. *Nat. Mater.* **3**, 862–867 (2004).
9. Yuasa, S., Nagahama, T., Fukushima, A., Suzuki, Y. & Ando, K. Giant room-temperature magnetoresistance in single-crystal Fe/MgO/Fe magnetic tunnel junctions. *Nat. Mater.* **3**, 868–71 (2004).
10. Ikeda, S., Miura, K., Yamamoto, H., Mizunuma, K., Gan, H. D., Endo, M., Kanai, S., Hayakawa, J., Matsukura, F. & Ohno, H. A perpendicular-anisotropy CoFeB-MgO magnetic tunnel junction. *Nat. Mater.* **9**, 721–4 (2010).
11. Ralph, D. C. & Stiles, M. D. Spin transfer torques. *J. Magn. Magn. Mater.* **320**, 1190–1216 (2008).
12. Brataas, A., Kent, A. D. & Ohno, H. Current-induced torques in magnetic materials. *Nat. Mater.* **11**, 372–81 (2012).
13. Miron, I. M., Garello, K., Gaudin, G., Zermatten, P.-J., Costache, M. V, Auffret, S., Bandiera, S., Rodmacq, B., Schuhl, A. & Gambardella, P. Perpendicular switching of a single ferromagnetic layer induced by in-plane current injection. *Nature* **476**, 189–193

- (2011).
14. Liu, L., Pai, C.-F., Li, Y., Tseng, H. W., Ralph, D. C. & Buhrman, R. A. Spin-Torque Switching with the Giant Spin Hall Effect of Tantalum. *Science* (80-.). **336**, 555–558 (2012).
 15. Matsukura, F., Tokura, Y. & Ohno, H. Control of magnetism by electric fields. *Nat. Nanotechnol.* **10**, 209–220 (2015).
 16. Wang, W.-G., Li, M., Hageman, S. & Chien, C. L. Electric-field-assisted switching in magnetic tunnel junctions. *Nat. Mater.* **11**, 64–68 (2012).
 17. Shiota, Y., Nozaki, T., Bonell, F., Murakami, S., Shinjo, T. & Suzuki, Y. Induction of coherent magnetization switching in a few atomic layers of FeCo using voltage pulses. *Nat. Mater.* **11**, 39–43 (2012).
 18. Grezes, C., Ebrahimi, F., Alzate, J. G., Cai, X., Katine, J. A., Langer, J., Ocker, B., Khalili, P. & Wang, K. L. Ultra-low switching energy and scaling in electric-field-controlled nanoscale magnetic tunnel junctions with high resistance-area product. **20**, 2–5 (2016).
 19. Kanai, S., Matsukura, F. & Ohno, H. Electric-field-induced magnetization switching in CoFeB/MgO magnetic tunnel junctions with high junction resistance. *Appl. Phys. Lett.* **108**, 192406 (2016).
 20. You, C. & Bader, S. Prediction of switching/rotation of the magnetization direction with applied voltage in a controllable interlayer exchange coupled system. *J. Magn. Magn. Mater.* **195**, 488–500 (1999).
 21. You, C. Y. & Suzuki, Y. Tunable interlayer exchange coupling energy by modification of Schottky barrier potentials. *J. Magn. Magn. Mater.* **293**, 774–781 (2005).
 22. Zhuravlev, M. Y., Vedyayev, a V & Tsymbal, E. Y. Interlayer exchange coupling across a ferroelectric barrier. *J. Phys. Condens. Matter* **22**, 352203 (2010).
 23. Fechner, M., Zahn, P., Ostanin, S., Bibes, M. & Mertig, I. Switching magnetization by 180 degree with an electric field. *Phys. Rev. Lett.* **108**, 1–5 (2012).
 24. Newhouse-Illige, T., Liu, Y., Xu, M., Reifsnyder Hickey, D., Kundu, A., Almasi, H., Bi, C., Wang, X., Freeland, J. W., Keavney, D. J., Sun, C. J., Xu, Y. H., Rosales, M., Cheng, X. M., Zhang, S., Mkhoyan, K. A. & Wang, W. G. Voltage-controlled interlayer coupling in perpendicularly magnetized magnetic tunnel junctions. *Nat. Commun.* **8**, 15232 (2017).
 25. Faure-Vincent, J., Tiusan, C., Bellouard, C., Popova, E., Hehn, M., Montaigne, F. & Schuhl, a. Interlayer Magnetic Coupling Interactions of Two Ferromagnetic Layers by Spin Polarized Tunneling. *Phys. Rev. Lett.* **89**, 107206 (2002).
 26. Bruno, P. Theory of interlayer magnetic coupling. *Phys. Rev. B* **52**, 411 (1995).

27. Slonczewski, J. C. Conductance and exchange coupling of two ferromagnets separated by a tunneling barrier. *Phys. Rev. B* **39**, 6995–7002 (1989).
28. Katayama, T., Yuasa, S., Velev, J., Zhuravlev, M. Y., Jaswal, S. S. & Tsymbal, E. Y. Interlayer exchange coupling in Fe/MgO/Fe magnetic tunnel junctions. *Appl. Phys. Lett.* **89**, 112503 (2006).
29. Moritz, J., Garcia, F., Toussaint, J. C., Dieny, B. & Nozières, J. P. Orange peel coupling in multilayers with perpendicular magnetic anisotropy: Application to (Co/Pt)-based exchange-biased spin-valves. *Europhys. Lett.* **65**, 123–129 (2007).
30. Nistor, L. E. *Magnetic tunnel junctions with perpendicular magnetization : anisotropy , magnetoresistance , magnetic coupling and spin transfer torque switching PhD diss.* (L'UNIVERSITÉ DE GRENOBLE, 2011).
31. Almasi, H., Xu, M., Xu, Y., Newhouse-Illige, T. & Wang, W. G. Effect of Mo insertion layers on the magnetoresistance and perpendicular magnetic anisotropy in Ta/CoFeB/MgO junctions. *Appl. Phys. Lett.* **109**, 32401 (2016).
32. Gallagher, W. J., Parkin, S. S. P., Lu, Y., Bian, X. P., Marley, a., Roche, K. P., Altman, R. a., Rishton, S. a., Jahnes, C., Shaw, T. M. & Xiao, G. Microstructured magnetic tunnel junctions (invited). *J. Appl. Phys.* **81**, 3741 (1997).
33. Bi, C., Liu, Y., Newhouse-Illige, T., Xu, M., Rosales, M., Freeland, J. W., Mryasov, O., Zhang, S., te Velthuis, S. G. E. & Wang, W. G. Reversible Control of Co Magnetism by Voltage-Induced Oxidation. *Phys. Rev. Lett.* **113**, 267202 (2014).
34. Bauer, U., Emori, S. & Beach, G. S. D. Voltage-controlled domain wall traps in ferromagnetic nanowires. *Nat. Nanotechnol.* **8**, 411–6 (2013).
35. Bauer, U., Yao, L., Tan, A., Agrawal, P., Emori, S., Tuller, H. L., Dijken, S. van & Beach, G. S. D. Magneto-ionic control of interfacial magnetism. *Nat. Mater.* **14**, 174 (2015).
36. Nowak, J. & Raułuszkiewicz, J. Spin dependent electron tunneling between ferromagnetic films. *J. Magn. Magn. Mater.* **109**, 79–90 (1992).
37. LeClair, P., Moodera, J. S. & Meservey, R. Ferromagnetic-ferromagnetic tunneling and the spin filter effect. *J. Appl. Phys.* **76**, 6546 (1994).
38. Gopman, D. B., Bedau, D., Wolf, G., Mangin, S., Fullerton, E. E., Katine, J. A. & Kent, A. D. Temperature dependence of the switching field in all-perpendicular spin-valve nanopillars. *Phys. Rev. B - Condens. Matter Mater. Phys.* **88**, 1–5 (2013).
39. Fu, Y., Barsukov, I., Li, J., Gonçalves, A. M., Kuo, C. C., Farle, M. & Krivorotov, I. N. Temperature dependence of perpendicular magnetic anisotropy in CoFeB thin films. *Appl. Phys. Lett.* **108**, 142403 (2016).
40. Miller, A. E., Jelinek, F. J., Gschneidner, K. A. & Gerstein, B. C. Low-Temperature

- Magnetic Behavior of Several Oxides of Gadolinium. *J. Chem. Phys.* **55**, 2647–2648 (1971).
41. Shang, C., Nowak, J., Jansen, R. & Moodera, J. Temperature dependence of magnetoresistance and surface magnetization in ferromagnetic tunnel junctions. *Phys. Rev. B* **58**, R2917–R2920 (1998).
 42. Julliere, M. Tunneling between ferromagnetic films. *Phys. Lett. A* **54**, 225–226 (1975).
 43. Teixeira, J. M., Ventura, J., Araujo, J. P., Sousa, J. B., Fernández-García, M. P., Wisniowski, P. & Freitas, P. P. Evidence of spin-polarized direct elastic tunneling and onset of superparamagnetism in MgO magnetic tunnel junctions. *Phys. Rev. B - Condens. Matter Mater. Phys.* **81**, 1–8 (2010).
 44. Yuan, L., Liou, S. & Wang, D. Temperature dependence of magnetoresistance in magnetic tunnel junctions with different free layer structures. *Phys. Rev. B* **73**, 134403 (2006).
 45. Xu, Y., Ephron, D. & Beasley, M. R. Directed inelastic hopping of electrons through metal-insulator-metal tunnel junctions. *Phys. Rev. B* **52**, 2843–2859 (1995).
 46. Glazman, L. I. & Matveev, K. A. Inelastic tunneling across thin amorphous films. *Sov. Phys. JETP* **67**, 1276–1282 (1988).
 47. Li, Z., Groot, C. de & Moodera, J. H. Gallium oxide as an insulating barrier for spin-dependent tunneling junctions. *Appl. Phys. Lett.* **77**, 3630 (2000).
 48. Yuasa, S. & Djayaprawira, D. D. Giant tunnel magnetoresistance in magnetic tunnel junctions with a crystalline MgO(0 0 1) barrier. *J. Phys. D: Appl. Phys.* **40**, R337–R354 (2007).
 49. Sukegawa, H., Mitani, S., Niizeki, T., Ohkubo, T., Inomata, K. & Hono, K. Epitaxial magnetic tunnel junctions with a monocrystalline Al₂O₃ barrier. *12th Jt. MMM-Intermag Conf. Abstr.* **AI-08**, (2013).
 50. Grunberg, P., Schreiber, R., Pang, Y., Brodsky, M. B. & Sowers, H. Layered Magnetic Structures: Evidence for Antiferromagnetic Coupling of Fe Layers across Cr Interlayers. *Phys. Rev. Lett.* **57**, 2442–5 (1986).
 51. Baibich, M. N., Broto, J. M., Fert, A., Van Dau, F. N., Petroff, F., Eitenne, P., Creuzet, G., Friederich, A. & Chazelas, J. Giant magnetoresistance of (001)Fe/(001)Cr magnetic superlattices. *Phys. Rev. Lett.* **61**, 2472–2475 (1988).
 52. Chiang, Y. F., Wong, J. J. I., Tan, X., Li, Y., Pi, K., Wang, W. H., Tom, H. W. K. & Kawakami, R. K. Oxidation-induced biquadratic coupling in Co/Fe/MgO/Fe(001). *Phys. Rev. B* **79**, 184410 (2009).
 53. Nistor, L. E., Rodmacq, B., Auffret, S., Schuhl, A. & Dieny, B. Antiferromagnetic

- Coupling in Sputtered MgO Tunnel Junctions With Perpendicular Magnetic Anisotropy. *Magn. IEEE Trans.* **45**, 3472–3475 (2009).
54. Nistor, L. E., Rodmacq, B., Auffret, S., Schuhl, A., Chshiev, M. & Dieny, B. Oscillatory interlayer exchange coupling in MgO tunnel junctions with perpendicular magnetic anisotropy. *Phys. Rev. B* **81**, 220407 (2010).
 55. Toscano, S., Briner, B. & Landolt, M. *Magnetism and Structure in systems of Reduced Dimensions*. (Plenum Press, 1993).
 56. Zhuravlev, M. Y., Tsymbal, E. Y. & Vedyayev, A. V. Impurity-assisted interlayer exchange coupling across a tunnel barrier. *Phys. Rev. Lett.* **94**, 1–4 (2005).
 57. Yang, H. X., Chshiev, M., Kalitsov, a., Schuhl, a. & Butler, W. H. Effect of structural relaxation and oxidation conditions on interlayer exchange coupling in Fe|MgO|Fe tunnel junctions. *Appl. Phys. Lett.* **96**, 262509 (2010).
 58. Néel, L. Magnetisme-sur un nouveau mode de couplage entre les animantations de deux couches minces ferromagnetiques. *Comptes Rendus Hebd. Des Seances L Acad. Des Sci.* **255**, 1676 (1962).
 59. Feng, G., Wu, H. C., Feng, J. F. & Coey, J. M. D. Temperature dependent coercivity crossover in pseudo-spin-valve magnetic tunnel junctions with perpendicular anisotropy. *Appl. Phys. Lett.* **99**, (2011).
 60. Geprägs, S., Meyer, S., Altmannshofer, S., Opel, M., Wilhelm, F., Rogalev, A., Gross, R. & Goennenwein, S. T. B. Investigation of induced Pt magnetic polarization in Pt/Y₃Fe₅O₁₂ bilayers. *Appl. Phys. Lett.* **101**, 262407 (2012).